CrystEngComm

PAPER

View Article Online
View Journal | View Issue

Structural and optical investigations of charge transfer complexes involving the F_4TCNQ dianion†

Cite this: *CrystEngComm*, 2014, **16**, 5234

Ashley L. Sutton,[a] Brendan F. Abrahams,*[a] Deanna M. D'Alessandro,[b] Robert W. Elliott,[a] Timothy A. Hudson,[a] Richard Robson*[a] and Pavel M. Usov[b]

Received 7th February 2014,
Accepted 20th April 2014

DOI: 10.1039/c4ce00289j

www.rsc.org/crystengcomm

7,7,8,8-Tetracyano-2,3,4,5-tetrafluoroquinodimethane (F_4TCNQ) in its dianionic form, F_4TCNQ^{2-}, is shown to form charge transfer complexes with a wide variety of organic cations. The structures and spectroscopic properties of fourteen F_4TCNQ^{2-} salts are described, thirteen of which have colours consistent with the formation of charge transfer complexes. Unlike neutral F_4TCNQ charge transfer complexes, the dianion, F_4TCNQ^{2-} is able to act as a donor in its interaction with suitable cations that serve as acceptors in solid-state complexes. The F_4TCNQ^{2-} salts described in this work have been categorised into five different structural types according to the relative arrangements of cations and anions. In each case, structural and IR spectroscopic data indicate that the anions retain a formal −2 charge upon formation of the salt. The optical band gaps, determined from Vis-NIR spectra, are found to have the lowest values when the cation is a viologen, either methyl viologen or diphenylmethyl viologen.

Introduction

The compound 7,7,8,8-tetracyanoquinodimethane (TCNQ) has been the focus of considerable attention because of its ability to act as an electron acceptor (A) in donor–acceptor charge transfer complexes (D–A).[1] This stable, quinoid-like molecule is able to undergo a one electron reduction to form a radical monoanion, $TCNQ^{-\bullet}$, which also exhibits good stability. In addition to the formal 0 and −1 oxidation states, investigations of charge transfer complexes indicate that TCNQ is able to carry a partial negative charge, a feature that has been linked to interesting physical properties such as electrical conductivity.[2] Perhaps the best known charge transfer complex incorporating TCNQ is TTF–TCNQ (TTF = tetrathiafulvalene) which forms a crystalline solid and is recognised as the first example of a purely organic electrical conductor.[3] In this structure the donor TTF molecules are arranged in infinite parallel stacks, which possess a positive charge whilst the acceptor TCNQ molecules are arranged in neighboring parallel stacks and carry a corresponding negative charge.

In addition to the single electron reduction to the radical anion form, TCNQ is also capable of undergoing a two electron reduction to form a dianion ($TCNQ^{2-}$) in which the 6-membered ring is aromatic.[4] The dianionic form was reported to be sensitive to aerial oxidation[5] and as a result received relatively little attention compared to the neutral and radical forms. We have discovered that the acid form of this dianion, $TCNQH_2$, is stable and a convenient starting material for making coordination polymers, if the deprotonation of the molecule occurs in the presence of metal ions.[6] Upon deprotonation, to form the dianion, the tetrahedral carbon atoms become trigonal. A wide range of coordination polymers have been synthesised in which the dianion links to four metal centres that lie at the corners of a rectangle.[6] Recently we have expanded the series of $TCNQ^{2-}$-based coordination networks to include coordination polymers involving F_4TCNQ^{2-}.[7] The effect of the electron withdrawing fluorine atoms is to stabilize the dianion and make it less susceptible to aerial oxidation.[8]

In addition to the coordination polymers, we reported in 2009 crystal structures of $TCNQ^{2-}$ salts, many of which were intensely coloured as a result of forming charge transfer complexes with cations.[9] Instead of TCNQ acting as the acceptor, as it does in charge transfer complexes such as TTF–TCNQ, it is in its fully reduced form, now playing the role of the donor.

The structural organization of the donor and acceptor components in charge-transfer complexes is known to significantly affect the physical properties of the solid.[10] Through an understanding of the factors that govern the structural arrangements of the components in a charge-transfer solid, some degree of control over the organization of donor and acceptor molecules in the crystalline state may be anticipated,

[a] *School of Chemistry, University of Melbourne, Victoria 3010, Australia*
[b] *School of Chemistry, University of Sydney, NSW 2006, Australia.*
E-mail: bfa@unimelb.edu.au, r.robson@unimelb.edu.au; Fax: +61 3 9347 5180

† Electronic supplementary information (ESI) available: Supplementary figures including powder diffraction patterns. CCDC 985158–985172. For ESI and crystallographic data in CIF or other electronic format see DOI: 10.1039/c4ce00289j

which in turn offers the prospect of tailoring the properties of charge-transfer solids. Numerous structural studies have been undertaken on charge-transfer complexes involving TCNQ acting as the acceptor, but very few have focused on the dianionic form of TCNQ where it plays the role of the donor.[11] This current work is directed towards an examination of the factors that govern the arrangement of the components when F_4TCNQ^{2-} is combined with a range of cations (**1–14**) that can act as potential acceptors in charge transfer solids.

Results and discussion

The salts of the F_4TCNQ^{2-} ion reported in this paper have been divided into five categories depending upon the arrangements of the cations and anions determined using single crystal X-ray diffraction. Schematic representations of the donor, D (F_4TCNQ^{2-}) and acceptor groups, A, in structural types I–IV are depicted in Fig. 1.

Type I – stacks consisting of alternating ions (DADADA)

In the type I packing arrangement, dianions (F_4TCNQ^{2-}) are arranged in infinite stacks with a cation or at least part of a cation located between F_4TCNQ^{2-} units. A neat example of this arrangement is provided by [(**1**)F_4TCNQ] which consists of stacks containing alternating F_4TCNQ^{2-} anions and methyl viologen (**1**) cations (Fig. 2). The DADADA arrangement of the donors, D (F_4TCNQ^{2-}) and acceptors, A, (methyl viologen), allows the cations and anions to participate in close contact face-to-face interactions on either side of each ion with separations between atoms of neighbouring ions as low as 3.2 Å. Interestingly, the long axis of the methyl viologen is inclined to the long axis of the F_4TCNQ dianion, as indicated in Fig. 2a.

When diphenylmethyl viologen (**2**) is used instead of methyl viologen, a type I structure is obtained but there are significant differences between [(**1**)F_4TCNQ] and [(**2**)F_4TCNQ]. As indicated in Fig. 3 face-to-face contact is made between alternating cations and anions within a stack but the stack is now "stepped". This stepped arrangement results in reasonably close contact between F_4TCNQ^{2-} anions belonging to neighbouring stacks.

The compound [(**3**)F_4TCNQ] is unlike other members of the type I group in that the cation does not contain an aromatic ring that is likely to serve as an acceptor in a charge transfer interaction *e.g.* a pyridinium ring or a phenyl ring with electron withdrawing substituents. As a result the absence of face-to-face interactions involving F_4TCNQ^{2-} and the cation is unsurprising. Nevertheless, as a type I structure, the stacks consist of alternating cations and anions (see ESI†).

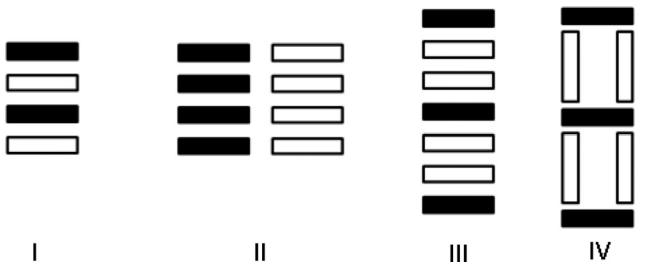

Fig. 1 Schematic representations of structural types I–IV. The black and white rectangles represent donor and acceptor groups respectively.

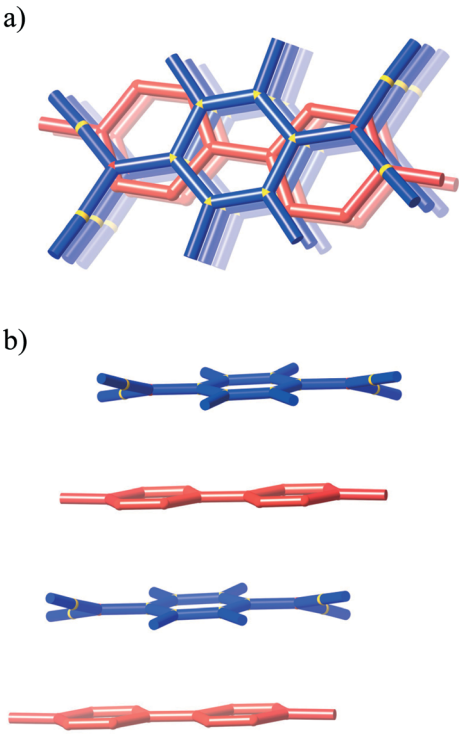

Fig. 2 Stick representations of [(**1**)F_4TCNQ] showing a single stack viewed a) along the stacking direction and b) almost normal to the stacking direction. The cation is indicated in red and the anion in blue.

The *m*-nitrobenzylpyridinium cation, **4**, is an elbow-shaped monocation that possesses two types of electron deficient aromatic rings either of which could potentially interact in a face-to-face manner with the F_4TCNQ^{2-} anion. In the compound [(**4**)$_2$(F_4TCNQ)]·0.5MeOH (Fig. 4) it is the nitrophenyl group that makes face-to-face contact with the F_4TCNQ^{2-} anion. In fact a pair of almost co-planar nitrophenyl groups are located between F_4TCNQ^{2-} anions within an infinite stack. An unusual feature of this structure is the manner in which the cations are arranged so as to produce an infinite "channel" with a cross-section resembling a parallelogram. The F_4TCNQ^{2-} anions are located within the channels as indicated in Fig. 4. The channel direction is almost normal to the stacking direction of the donor and acceptor groups.

Cation **5** closely resembles cation **4**, the difference being that there are now two nitro groups bound to the phenyl ring instead of one. As with [(**4**)$_2$(F_4TCNQ)]·0.5MeOH, the elbow-shaped cations in [(**5**)$_2$(F_4TCNQ)] are arranged so as to form infinite channels that have a cross-section resembling a parallelogram. Whilst pairs of nitrophenyl groups, sandwiched between F_4TCNQ^{2-} anions in [(**4**)$_2$(F_4TCNQ)]·0.5MeOH, are close to co-planar the corresponding dinitrophenyl groups in [(**5**)$_2$(F_4TCNQ)] are parallel but not co-planar.

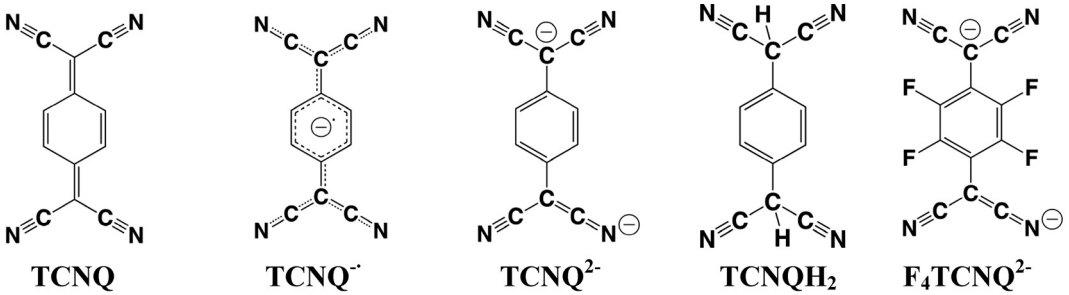

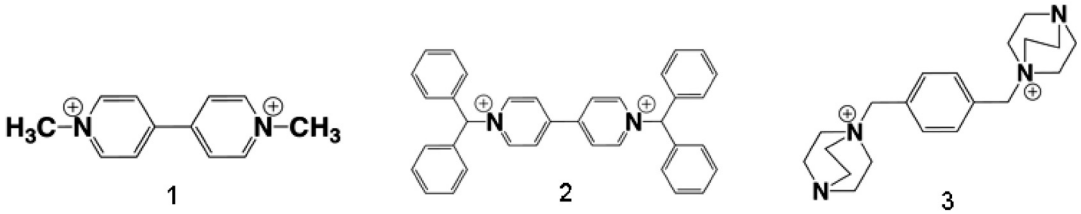

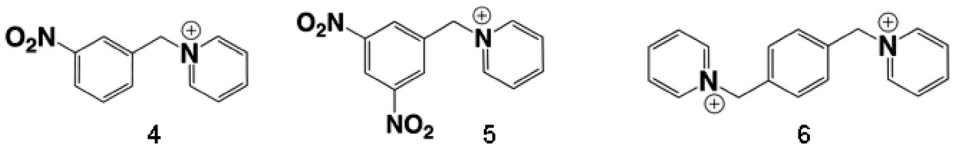

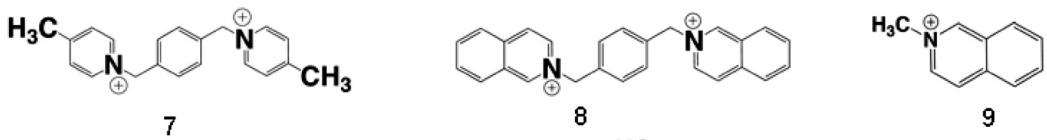

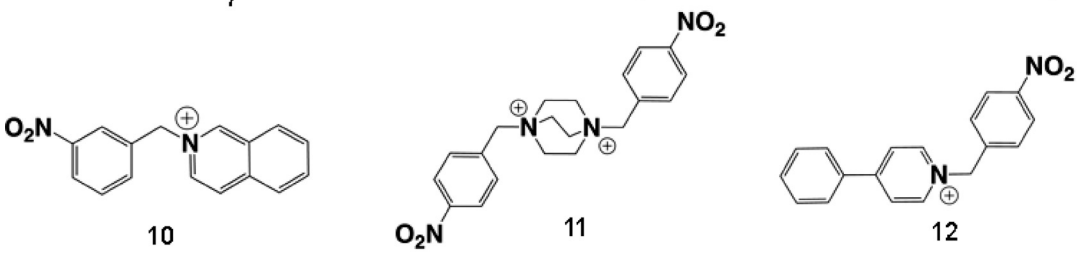

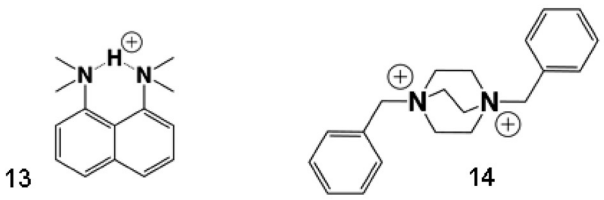

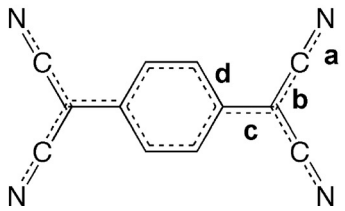

Scheme 1

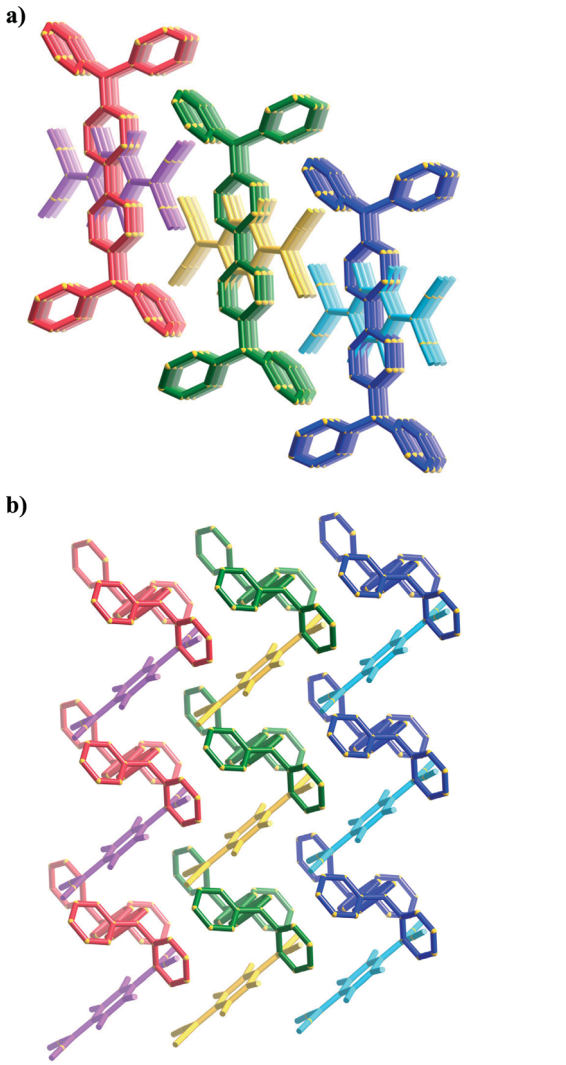

Fig. 3 Stick representations of [(**2**)F_4TCNQ] showing three cations and anions in three separate stacks (red and pink, green and yellow, and blue and aqua) viewed a) along the stacking direction and b) almost normal to the stacking direction.

Type II – segregated stacks of cations and anions (DDDDD and AAAAA)

The type II packing arrangement, with discrete stacks of dianionic F_4TCNQ and dication (DDDDD and AAAAA), was revealed for complexes [(**6–8**)(F_4TCNQ)]. The structure of [(**6**)(F_4TCNQ)] is presented in Fig. 5, which shows stacks of the dipyridylxylene cations and separate parallel stacks of the F_4TCNQ^{2-} anions. The separation between the centroids of neighboring F_4TCNQ^{2-} rings within a stack is 3.73 Å whilst the interplanar separation of the rings is 3.50 Å. The formation of these stacks is somewhat surprising given that one would expect repulsion between the like-charged ions. However, as inspection of Fig. 5a reveals, the orientation of the ions within a stack alternates in a manner that may be expected to reduce the repulsion between neighboring ions. The arrangement of the stacks is indicated in Fig. 5b.

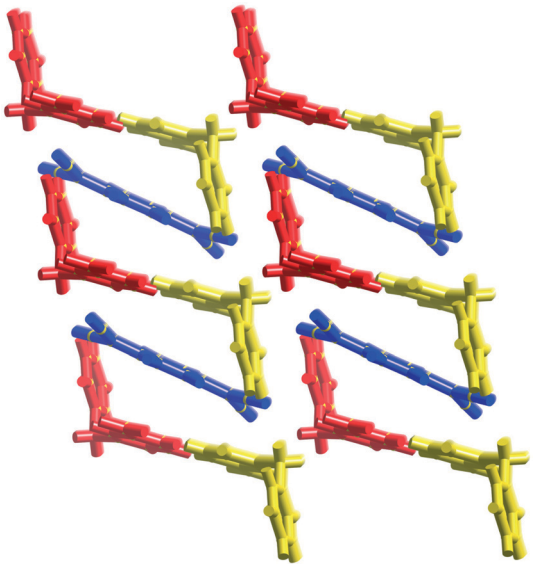

Fig. 4 A stick representation of [(**4**)$_2$$F_4$TCNQ] showing the formation of "channels" by elbow-shaped cations (red and gold) and the location of F_4TCNQ^{2-} anions (blue) within the channels. The channels extend into the page.

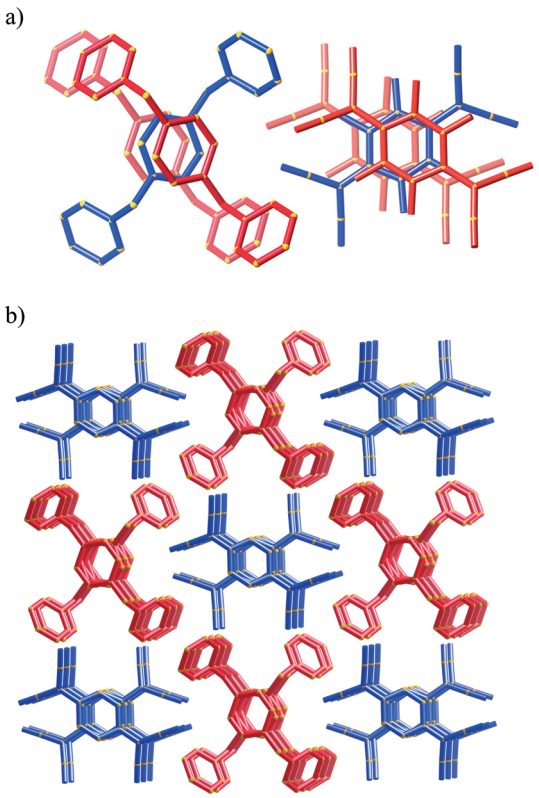

Fig. 5 Stick representations of [(**6**)F_4TCNQ] showing a) the alternation in orientation of the cations and anions within segregated stacks; ions are coloured red and blue depending upon their orientation and b) the arrangement of the segregated stacks (cations red, anions blue).

The structure of [(**7**)F_4TCNQ], which is represented in the ESI,† also has segregated stacks of cations and anions, however there are some interesting contrasts with [(**6**)(F_4TCNQ)]

which appear a little surprising given that the only difference between the cations is the presence of methyl groups. In [(7)F_4TCNQ] adjacent ions within either the cation or anion stack have the same orientation and are related by a pure translation along the stacking direction. In addition, the mean planes of the F_4TCNQ^{2-} anions in [(7)F_4TCNQ] are much more inclined to the stacking direction than that found in [(6)F_4TCNQ]. The separation between the centroids of neighboring F_4TCNQ^{2-} rings within a stack is 5.00 Å whilst the interplanar separation of the rings is 3.32 Å. The arrangement of anions and cations within stacks in [(8)F_4TCNQ] resembles that found in [(7)F_4TCNQ] (see ESI†). In the case of [(8)F_4TCNQ] the separation between the centroids of neighboring F_4TCNQ^{2-} rings within a stack is 5.41 Å whilst the interplanar separation of the rings is 3.01 Å.

Type III structures – DAADAADAAD stacks

The compounds [(**9**)$_2F_4$TCNQ] and [(**10**)$_2F_4$TCNQ] consist of discrete infinite stacks in which pairs of monocations are located either side of the F_4TCNQ^{2-} anion. Each cation in [(**9**)$_2F_4$TCNQ] makes face-to-face contact with a centrosymmetrically-related cation while each dianion, located on a centre of symmetry, makes contact with a pair of monocations. The orientation of the cations alternates along the stack as indicated in Fig. 6. Similar packing is apparent in [(**10**)$_2F_4$TCNQ] even though the cation now has a *meta*-nitrobenzyl group in place of the methyl group (see ESI†). It is interesting to note that the dianions in [(**10**)$_2F_4$TCNQ] prefer to participate in face-to-face interactions with the isoquinolinium group rather than the nitrophenyl group. This is in contrast to cations **4** and **5** where the nitrophenyl or dinitrophenyl groups rather than the pyridinium group preferentially associate with the dianion. The arrangement of cations and anions in [(**9**)$_2F_4$TCNQ] and [(**10**)$_2F_4$TCNQ] is similar to that found in the previously reported charge transfer salt {[Fe(C_5Me_5)$_2$]F_4TCNQ}.[11]

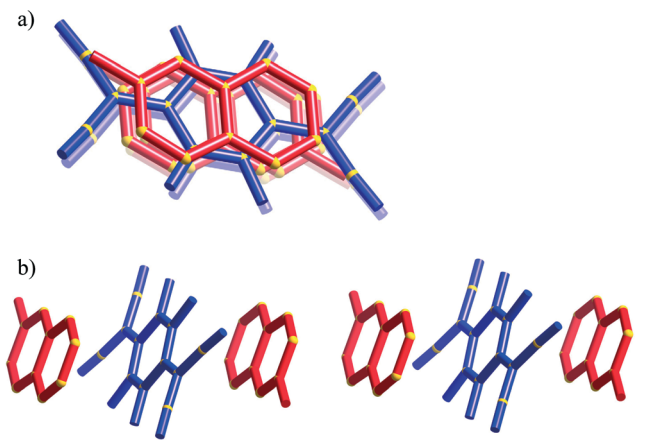

Fig. 6 Stick representations of [(**9**)$_2F_4$TCNQ] showing views a) along the stacking direction and b) almost normal to the stacking direction; cations are red, anions are blue.

The final member of the type III group is [(**11**)F_4TCNQ]. Unlike **9** and **10**, **11** is a dication and spans a pair of stacks. With the cations linking pairs of stacks a beautiful 2D network is generated (Fig. 7). As with [(**9**)$_2F_4$TCNQ] and [(**10**)$_2F_4$TCNQ] the dianion is located on a centre of symmetry; a centre of a symmetry is also located between the nitrobenzyl groups.

Type IV DAADAADAAD stacks with edge-to-face interactions between cations and anions

The type IV structures [(**12**)$_2F_4$TCNQ] and [(**13**)$_2F_4$TCNQ], show a somewhat surprising arrangement of the cations and anions. The compound [(**12**)$_2F_4$TCNQ] shares similarities with the type III structures in that there are stacks involving pairs of cations lying between F_4TCNQ^{2-} anions; however the cations, which do form face-to-face interactions with each other, form only edge-to-face interactions with the F_4TCNQ^{2-} anions within a stack as indicated in Fig. 8a. Within the crystal structure it is also possible to also identify stacks almost normal to those depicted in Fig. 8a, but in which the mean plane of the F_4TCNQ^{2-} anion is parallel with the stacking direction as indicated in Fig. 8b. In this stack the F_4TCNQ^{2-} anions form edge-to-face interactions with the cations. The compound [(**12**)$_2H_4$TCNQ] adopts a very similar structure to the fluorinated analogue [(**12**)$_2F_4$TCNQ].

[(**13**)$_2F_4$TCNQ] contains stacks extending in a direction almost normal to the mean plane of the F_4TCNQ^{2-} anion in which pairs of cations form edge-to-face interactions with the dianion (see ESI†). Unlike [(**12**)$_2F_4$TCNQ] however, there are no stacks in which the dianions form edge-to-face interactions with cations.

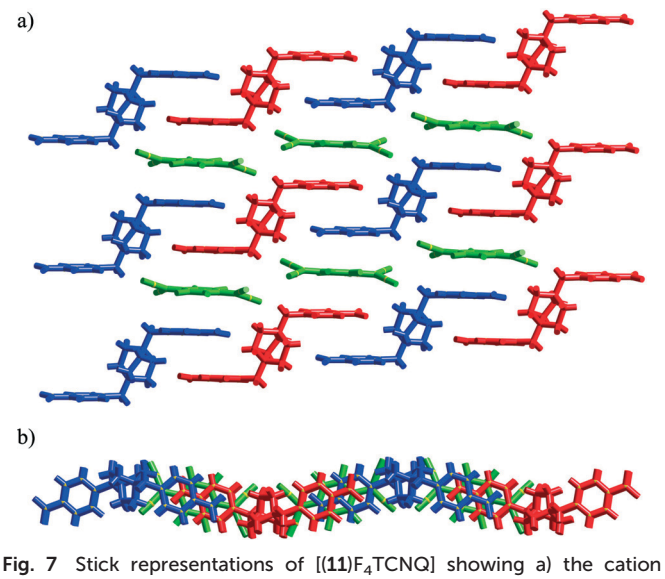

Fig. 7 Stick representations of [(**11**)F_4TCNQ] showing a) the cation spanning a pair of stacks and b) the resulting 2D π-stacked network viewed along the stacking direction. Cations are red and blue, F_4TCNQ^{2-} anions are green.

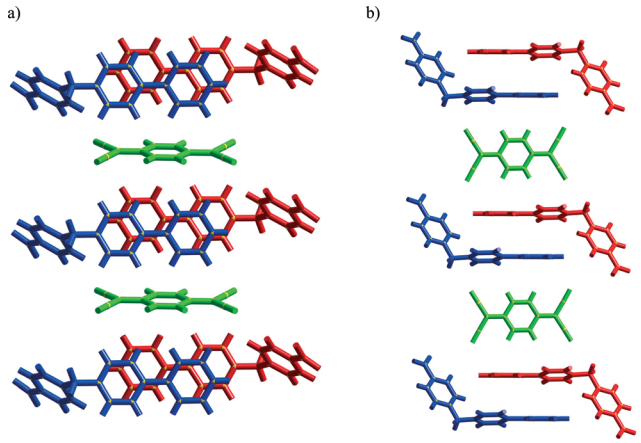

Fig. 8 Stick representations of the stacking arrangements in [(**12**)$_2$F$_4$TCNQ]. a) A stack in which pairs of cations form edge-to-face interactions with F_4TCNQ^{2-} anions. b) A stack in which F_4TCNQ^{2-} anions form edge-to-face interactions with cations. The two types of stacks intersect each other.

Type V – isolated F_4TCNQ^{2-} pairs

The final structure considered in this series concerns the compound, [(**14**)$_2$F$_4$TCNQ]·MeOH in which F_4TCNQ^{2-} anions associate with symmetry-related anions in a face-to-face interaction. The resulting pair of anions is well isolated from other pairs by the large dibenzyldabco cations (see ESI†).

General structural comments

The two –C(CN)$_2$ groups of each F_4TCNQ^{2-} anion considered in this series of compounds are close to co-planar, however some variation in the rotation of the aromatic ring along the long axis of the dianion is apparent. In each case the four nitrogen atoms lie close to the corners of a rectangle with long edge lengths in the range of 8.52–8.83 Å. The longer lengths (~8.8 Å) correspond to cases where the whole anion is close to planar. The relationship reflects the steric influence of the fluorine atoms; when they are in the same plane as the two –C(CN)$_2$ groups the nitrogen atoms lying at the corners of a long length of the rectangle are forced further apart. A consequence of the nitrogen atoms located on the long edge being forced further apart is a contraction along the short edge of the rectangle. The separation between nitrogen atoms defining the short edge of the rectangle spans 4.16 to 4.38 Å. The shorter length for this particular separation corresponds to cases in which the whole anion is close to planar. The rotation of the aromatic ring relative to the mean plane of the –C(CN)$_2$ groups for each dianion is given in Table 1.

The structures investigated within this series of compounds provide an interesting comparison with the structures of charge transfer solids involving the TCNQ dianion. The TCNQ analogues of [(**1**)F$_4$TCNQ], [(**2**)F$_4$TCNQ] and [(**6**)F$_4$TCNQ] have been previously reported[9] and the compound [(**12**)$_2$TCNQ] is reported in this work. As with [(**1**)F$_4$TCNQ] and [(**2**)F$_4$TCNQ], [(**1**)TCNQ] and [(**2**)TCNQ] adopt type I structures and both [(**12**)$_2$F$_4$TCNQ] and [(**12**)$_2$TCNQ] adopt type III structures. Interestingly, [(**6**)F$_4$TCNQ] adopts a type II structure with the segregated stacks whereas [(**6**)TCNQ] has a type I structure with the alternating cations and anions in the same stack. Although the F$_4$TCNQ dianionic structures tend to exhibit a greater deviation from planarity, the TCNQ dianions are not always planar.

The Kistenmacher relationship is an empirical relationship that provides an estimation of the charge on F$_4$TCNQ by considering certain bond lengths within the molecule.[10a] The relationship between the estimated charge and bond distances for F$_4$TCNQ is given by the expression:

Table 1 Structural and spectroscopic data

Packing type	Compound	Colour	ν_{CN} (cm^{-1})	$c/(b+d)$	Estimated charge[a]	Optical band gap (eV)	Dihedral angle[b] (°)
I	[(**1**)(F$_4$TCNQ)]	Dark green	2172, 2142	0.520	−1.93(6)	1.08	18.1
	[(**2**)(F$_4$TCNQ)]	Black/brown	2164, 2131	0.519	−1.94(17)	0.817	4.6
	[(**3**)(F$_4$TCNQ)]	Green	2164, 2132	0.524	−2.14(11)	2.83	3.3
	[(**4**)$_2$(F$_4$TCNQ)]·0.5MeOH	Blue/purple	2165, 2129	0.518	−1.86(7)	1.78	12.7
	[(**5**)$_2$(F$_4$TCNQ)]	Black	2172, 2158	0.522	−2.05(8)	1.50	2.7
II	[(**6**)(F$_4$TCNQ)]	Red/orange	2161, 2132	0.523	−2.09(6)	2.30	32.8
	[(**7**)(F$_4$TCNQ)]	Red	2157, 2121	0.518	−1.86(17)	2.05	17.1
	[(**8**)(F$_4$TCNQ)]	Dark red	2164, 2131	0.521	−2.01(6)	2.73	29.6
III	[(**9**)$_2$(F$_4$TCNQ)]	Dark green	2159, 2123	0.521	−1.97(6)	1.67	7.2
	[(**10**)$_2$(F$_4$TCNQ)]	Dark purple	2165, 2134	0.522	−2.02(7)	1.75	27.1
	[(**11**)(F$_4$TCNQ)]	Black	2162, 2124	0.519	−1.90(8)	1.45	17.1
IV	[(**12**)$_2$(H$_4$TCNQ)]	Purple	2155, 2108	0.521	−1.88(5)	1.85	1.2
	[(**12**)$_2$(F$_4$TCNQ)]	Dark green	2166, 2135	0.519	−1.91(5)	1.50	4.9
	[(**13**)$_2$(F$_4$TCNQ)]	Yellow	2166, 2131	0.521	−1.99(8)	2.89	26.8
V	[(**14**)$_2$(F$_4$TCNQ)$_2$]·MeOH	Pale yellow	2164, 2133	0.523	−2.14(17)	2.63	9.1
				0.528	−2.29(17)		28.7

[a] The charge, q, is estimated using the Kistenmacher relationship $q = A[c/(b+d)] + B$. For F$_4$TCNQ $A = -45.756$ and $B = 21.846$; for TCNQ $A = -41.667$ and $B = 19.818$; b, c and d refer to the lengths of bonds indicated in Scheme 1. Values for A and B were calculated as indicated in the ESI. [b] The dihedral angle represents the rotation of the aromatic ring relative to the mean plane of the –C(CN)$_2$ groups for the anions.

$$q = -45.756[c/(b + d)] + 21.846$$

where q is the estimated charge and b, c and d are bond lengths indicated in Scheme 1. The co-efficients used in this equation were calculated as indicated in the ESI.† The estimated charge, q, on the anion in each of the F_4TCNQ structures (Table 1) is consistent with the anion existing in its formal −2 state. The ν_{CN} stretching frequencies, which are also presented in Table 1 provide further support for the −2 charge assignment for the F_4TCNQ dianion. For neutral and monoanionic forms of F_4TCNQ, typical ν_{CN} values are in the region 2227[12] and 2197, 2178 cm^{-1} (ref. 13) respectively whilst for the dianion the ν_{CN} stretching frequencies are commonly ~2167, 2133 cm^{-1}.[11]

Optical band gap measurements

All of the F_4TCNQ^{2-} compounds reported in the current work except for the type V compound, [(**14**)$_2F_4$TCNQ]·MeOH, strongly absorb in the visible region although there is significant variation in the intensity and the colours of the compounds, as indicated in Table 1. Thus while the anion may be formally assigned a −2 oxidation state on the basis of the Kistenmacher relationship and the ν_{CN} stretching frequencies, it is reasonable to assume that charge transfer interactions are present in all of the examples described above (except for [(**14**)$_2F_4$TCNQ]·0.5MeOH) given that the individual component ions do not display significant absorption in the visible region. Vis-NIR measurements are a particularly useful tool for investigating such charge transfer solids as they may be employed to generate a Tauc plot that allows the determination of an optical band gap.

The solid-state diffuse reflectance spectrum for [(**1**)F_4TCNQ] is presented in Fig. 9a and the corresponding Tauc plot[14] is shown in Fig. 9b. The spectra and corresponding Tauc plots for the remaining compounds are presented in the ESI.† The optical band gap determined for each of the compounds is presented in Table 1. Of particular note are the relatively low optical band gaps found for [(**1**)F_4TCNQ] and [(**2**) F_4TCNQ] of 1.08 and 0.82 eV respectively. These are significantly lower values than those found for the other complexes (1.45–2.89 eV). Whilst both of these compounds adopt type I packing arrangements, *i.e.* DADADA stacks, other members of this group have significantly higher optical band gaps. Large ranges in the optical band gaps are also apparent in the other structural types and thus it would appear that the packing arrangements themselves are not a strong indicator for the size of the optical band gap. It is however significant that the compounds with the two lowest optical band gaps have viologen cations as the counterions. Viologens are well known electron acceptor cations and it would appear that they are particularly well-suited to playing this role in [(**1**)F_4TCNQ] and the closely related compound [(**2**)F_4TCNQ]. Although the Kistenmacher relationship provides only a crude estimate of charge on the anion it is interesting to note that in both compounds the magnitude of the charge is less than 2 suggesting that the charge on the donor F_4TCNQ^{2-} is delocalized onto the cationic viologen acceptors resulting in the reduced band gap.

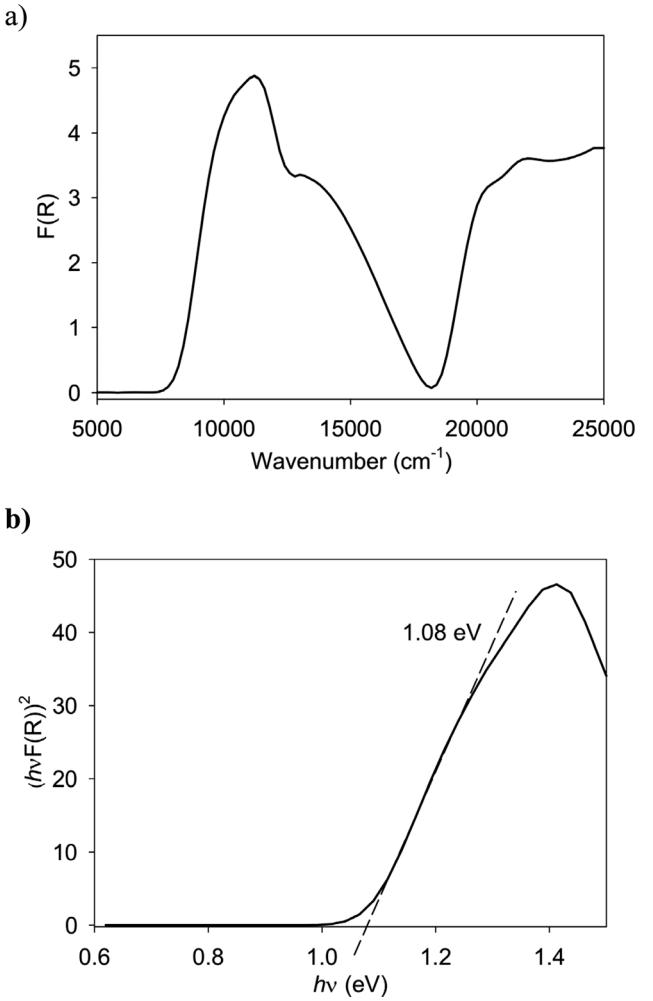

Fig. 9 a) The Vis-NIR solid-state diffuse reflectance spectrum of [(**1**)F_4TCNQ]. b) The Tauc plot derived from the spectrum showing the estimation of the optical band gap.

Conclusion

The structures of 14 compounds involving the dianion, F_4TCNQ^{2-}, have been elucidated and categorised according to the relative arrangements of the ions. The most common arrangement, type I, involves a simple alternation of cation and anion within infinite parallel stacks in which there are face-to-face interactions between oppositely charged ions. Of particular importance within this group of structures are [(**1**)F_4TCNQ] and [(**2**)F_4TCNQ] in which the cation is a viologen. These two compounds exhibit the lowest optical band gaps of any compounds reported in this work. It is noted that other compounds with similar packing arrangements (*i.e.* type I) exhibit optical band gaps that are much higher and thus the electronic nature of the cation rather

than the packing arrangement would appear to be a dominant influence on the optical band gap. Segregated parallel stacks of cations and anions are apparent in the type II structures. Whilst a similar arrangement is found in the organic conductor TTF–TCNQ, unexceptional optical band gaps were found for the compounds in this group. Type III and type IV structures are similar to type I structures except that pairs of acceptor units are located between the F_4TCNQ^{2-} anions. In the type III structures there are face-to-face interactions between the cations and the anions whereas in the type IV structures the dianions form an edge-to-face interaction with the cation. The final structural type, type V, only has one member and consists of an unusual structure in which the dianions form weakly associated face-to-face dimers. These dimers are separated from each other by the bulky cation.

Perhaps the most surprising aspect of this structural investigation is the close association of the dianions in the type II structures. As indicated above, the anion clearly carries a −2 charge and yet prefers to form face-to-face interactions with two dianions (above and below). Segregated stacks are not unprecedented and are a feature of the TTF–TCNQ structure, however the net magnitude of the charge on each cation and anion is less than one in TTF–TCNQ. Presumably the arrangement in the type II structures reflects the location of the charges near the periphery of both the anions and the cations allowing for a favourable electrostatic attraction between members of neighbouring stacks. Similar considerations may provide an explanation for the close association of the dianions in the type V structure.

Experimental

Synthesis of F_4TCNQH_2

F_4TCNQH_2 was prepared according to the literature method using 2,3,5,6-tetrafluoro-1,4-bis(*t*-butyldicyanomethyl)benzene as a starting material.[15]

Synthesis of [(1)(F_4TCNQ)]

A solution of [**1**]Cl_2 (18.0 mg, 0.07 mmol) and Li(OAc)·$2H_2O$ (18.4 mg, 0.18 mmol) in methanol (2 mL) was layered onto a solution of F_4TCNQH_2 (20.0 mg, 0.07 mmol) in DMF (1 mL). Dark green crystals of [(**1**)(F_4TCNQ)] separated from the solution overnight (1.9 mg, 6%). Elemental analysis calcd $C_{24}H_{14}F_4N_6$: C, 62.34; H, 3.05; N, 18.17; found: C, 62.56; H, 3.09; N, 18.43%. IR (KBr): 3049, 2172, 2142, 1638, 1481, 1228, 1138, 960, 837, 784, 549 cm^{-1}. Complexes [(**3**)(F_4TCNQ)], [(**6**)(F_4TCNQ)] and [(**11**)(F_4TCNQ)] were synthesised using the same general procedure with further details available in the ESI.†

Synthesis of [(4)$_2$(F_4TCNQ)]·0.5MeOH

To a solution of F_4TCNQH_2 (8.3 mg, 0.03 mmol) and Li(OAc)·$2H_2O$ (8.2 mg, 0.08 mmol) in methanol (2 mL) was added a solution of [**4**]Br (8.9 mg, 0.03 mmol) in methanol (2 mL). Upon slow evaporation blue/purple crystals of [(**4**)$_2$(F_4TCNQ)]·0.5MeOH formed from the solution (0.5 mg, 5%). Elemental analysis calcd $C_{73}H_{44}F_8N_{16}O_9$: C, 60.84; H, 3.08; N, 15.55; found: C, 60.80; H, 3.33; N, 15.49%. IR (KBr): 3442, 3065, 2922, 2165, 2129, 2104, 1631, 1523, 1489, 1346, 1229, 1142, 961, 733, 704, 672 cm^{-1}. Complexes [(**2**)(F_4TCNQ)], [(**5**)$_2$(F_4TCNQ)], [(**7**)(F_4TCNQ)], [(**8**)(F_4TCNQ)], [(**9**)$_2$(F_4TCNQ)], [(**10**)$_2$(F_4TCNQ)], [(**12**)$_2$(H_4TCNQ)], [(**12**)$_2$(F_4TCNQ)] and [(**14**)$_2$(F_4TCNQ)$_2$·MeOH] were synthesised using the same general procedure with further details available in the ESI.†

Synthesis of [(13)$_2$(F_4TCNQ)]

To a suspension of F_4TCNQH_2 (8.3 mg, 0.03 mmol) in methanol (2 mL) was added a solution of 1,8-bis(dimethylamino)naphthalene (the unprotonated, neutral form of [**13**]) (6.4 mg, 0.03 mmol) in methanol (2 mL); the resultant mixture was heated with stirring, allowing evaporation to occur until the volume of the solution had approximately halved. Upon cooling yellow crystals of [(**13**)$_2$(F_4TCNQ)] separated from the solution overnight (4.8 mg, 45%). IR (KBr): 3007, 2922, 2166, 2131, 1484, 1188, 929, 772, 486 cm^{-1}.

Single crystal X-ray diffraction

Data were collected for all complexes on an Oxford Diffraction Supernova diffractometer using CuKα radiation, except for [(**2**)(F_4TCNQ)] and [(**14**)$_2$(F_4TCNQ)$_2$·MeOH] which were collected on an Oxford Diffraction Xcalibur Sapphire3 diffractometer using CuKα radiation. In general, crystals were transferred directly from the mother liquor to a protective oil before being mounted on the diffractometer in a stream of nitrogen at 130 K, with the exception of [(**14**)$_2$(F_4TCNQ)$_2$·MeOH] which was placed in a stream of nitrogen at 240 K. Structures were solved by direct methods and refined using a full matrix least-squares procedure based on F^2 (SHELX97).[16] The crystallographic analyses were performed using the WinGX system of programs.[17] Crystal data and refinement details are presented in Table 2.

Powder diffraction

Powder-XRD data for all complexes were collected on an Oxford SuperNova diffractometer using CuKα radiation, λ = 1.5418 Å. For all complexes the powder diffraction pattern of the bulk product matched the calculated diffraction pattern obtained from the single crystal structure determination. The measured and calculated powder patterns are presented in the ESI.†

Infrared spectra

Infrared spectra were collected on a Bruker Tensor 27 FT-IR using pressed KBr discs.

Solid state Vis-NIR spectroscopy

Vis-NIR diffuse reflectance spectroscopy was used to analyse powdered samples. Spectra were collected on a CARY 5000

Table 2 Crystal structure and refinement details

Compound	[(1)(F_4TCNQ)]	[(2)(F_4TCNQ)]	[(3)(F_4TCNQ)]	[(4)$_2$(F_4TCNQ)]·0.5MeOH	[(5)$_2$(F_4TCNQ)]	[(6)(F_4TCNQ)]
Formula	$C_{24}H_{14}F_4N_6$	$C_{48}H_{30}F_4N_6$	$C_{32}H_{32}F_4N_8$	$C_{36.5}H_{22}F_4N_8O_{4.5}$	$C_{36}H_{20}F_4N_{10}O_8$	$C_{30}H_{18}F_4N_6$
Crystal system	Monoclinic	Triclinic	Monoclinic	Triclinic	Triclinic	Monoclinic
Space group	$P2_1/n$	$P\bar{1}$	$C2/m$	$P\bar{1}$	$P\bar{1}$	$C2/c$
a (Å)	11.3750(3)	7.2739(9)	13.4546(11)	8.0153(4)	8.2034(5)	18.3535(5)
b (Å)	7.1927(2)	8.9106(11)	11.4276(10)	10.5291(7)	10.8428(10)	18.1472(5)
c (Å)	12.4527(3)	14.8749(18)	9.1962(9)	11.0731(7)	10.9912(10)	7.4618(2)
α (°)	90	105.302(10)	90	73.207(5)	95.047(7)	90
β (°)	93.830(2)	98.243(10)	101.490(8)	69.339(5)	109.560(7)	101.507(2)
γ (°)	90	102.661(10)	90	74.309(5)	108.643(7)	90
Cell volume (Å^3)	1016.57(5)	886.34(19)	1385.6(2)	822.17(9)	851.81(12)	2435.31(11)
Z	2	1	2	1	1	4
Reflections collected	5898	5084	2516	5420	5597	6007
Independent reflections	1829	3167	1376	3211	3054	2189
Parameters	155	262	112	240	262	181
R_1 [$I > 2\sigma(I)$]	0.0330	0.0636	0.0523	0.0472	0.0383	0.0333
wR_2 (all data)	0.0917	0.211	0.1557	0.1385	0.1076	0.0940

Compound	[(7)(F_4TCNQ)]	[(8)(F_4TCNQ)]	[(9)$_2$(F_4TCNQ)]	[(10)$_2$(F_4TCNQ)]	[(11)(F_4TCNQ)]	[(12)$_2$(H_4TCNQ)]
Formula	$C_{32}H_{22}F_4N_6$	$C_{38}H_{22}F_4N_6$	$C_{32}H_{20}F_4N_6$	$C_{44}H_{26}F_4N_8O_4$	$C_{32}H_{24}F_4N_8O_4$	$C_{24}H_{17}N_4O_2$
Formula weight	566.56	638.62	564.54	806.73	660.59	393.42
Temp (K)	130	130	130	130	130	130
Crystal system	Monoclinic	Triclinic	Monoclinic	Triclinic	Monoclinic	Triclinic
Space group	$P2_1/c$	$P\bar{1}$	$P2_1/n$	$P\bar{1}$	$C2/c$	$P\bar{1}$
a (Å)	5.0039(3)	5.4139(5)	6.5110(3)	9.1726(5)	10.2589(2)	8.0055(5)
b (Å)	15.2708(8)	10.4083(11)	16.6335(6)	10.6903(6)	12.2242(2)	8.5844(5)
c (Å)	16.7605(10)	13.9398(17)	11.4633(4)	10.7126(6)	22.2473(5)	15.3367(8)
α (°)	90	104.240(10)	90	73.150(5)	90	74.027(5)
β (°)	95.417(6)	98.724(9)	94.157(3)	80.841(5)	95.290(2)	88.077(5)
γ (°)	90	104.128(9)	90	64.809(5)	90	67.144(6)
Cell volume (Å^3)	1275.01(13)	719.36(13)	1238.22(8)	908.96(9)	2778.08(9)	930.52(9)
Z	2	1	2	1	4	2
Reflections collected	3778	4560	4660	6278	4971	6159
Independent reflections	3778	2720	2356	3546	2633	3649
Parameters	191	217	191	271	217	271
R_1 [$I > 2\sigma(I)$]	0.0948	0.0401	0.0436	0.0404	0.0457	0.0372
wR_2 (all data)	0.2812	0.1156	0.1304	0.1092	0.132	0.1007

Compound	[(12)$_2$(F_4TCNQ)]	[(13)$_2$(F_4TCNQ)]	[(14)$_2$(F_4TCNQ)$_2$·MeOH]
Formula	$C_{24}H_{15}F_2N_4O_2$	$C_{40}H_{38}F_4N_8$	$C_{61}H_{56}F_8N_{16}O$
Formula weight	429.4	706.79	1181.22
Temp (K)	130	130	240
Crystal system	Triclinic	Triclinic	Triclinic
Space group	$P\bar{1}$	$P\bar{1}$	$P\bar{1}$
a (Å)	8.1317(4)	8.6578(7)	12.9040(10)
b (Å)	9.0430(5)	9.6463(6)	13.3891(8)
c (Å)	15.1631(7)	11.6657(7)	19.1890(12)
α (°)	96.300(4)	109.413(6)	76.376(5)
β (°)	98.584(4)	101.096(6)	75.564(6)
γ (°)	116.492(5)	92.685(6)	65.911(6)
Cell volume (Å^3)	966.98(8)	895.22(11)	2897.3(3)
Z	2	1	2
Reflections collected	6526	5246	19 887
Independent reflections	3770	3033	10 408
Parameters	289	243	777
R_1 [$I > 2\sigma(I)$]	0.0336	0.0473	0.0657
wR_2 (all data)	0.0898	0.1334	0.2157

UV-Vis-NIR spectrophotometer with a Harrick Omni Diff Probe attachment using Varian WinUV software V3.0. The data were recorded from 5000 to 25 000 cm^{-1} with a scan rate of 6000 cm^{-1} min^{-1}. Samples were supported on high density filter paper which was also used to provide the background reference. Spectra are reported Kubelka–Munk transform, where $F(R) = (1 - R)^2/2R$ (R is the diffuse reflectance of the sample as compared to the background reference).

Elemental analysis

Elemental microanalyses were performed by the Campbell Microanalytical Laboratory Dunedin, New Zealand.

Acknowledgements

We gratefully acknowledge the financial support of the Australian Research Council.

References

1 K. P. Goetz, D. Vermeulen, M. E. Payne, C. Kloc, L. E. McNeil and O. D. Jurchescu, *J. Mater. Chem. C*, 2014, **2**, 3065, and references therein.

2 (*a*) J. B. Torrance, *Acc. Chem. Res.*, 1979, **12**, 79; (*b*) Z. Zhang, H. Zhao, H. Kojima, T. Mori and K. R. Dunbar, *Chem. - Eur. J.*, 2013, **19**, 3348; (*c*) R. A. Heintz, H. Zhao, X. Ouyang, G. Grandinetti, J. Cowen and K. R. Dunbar, *Inorg. Chem.*, 1999, **38**, 144; (*d*) N. Lopez, H. Zhao, A. Ota, A. V. Prosvirin, E. W. Reinheimer and K. R. Dunbar, *Adv. Mater.*, 2010, **22**, 986.

3 (*a*) J. Ferraris, D. O. Cowan, V. Walatka and J. H. Perlstein, *J. Am. Chem. Soc.*, 1973, **95**, 948; (*b*) M. Cohen, L. Coleman, A. Garito and A. Heeger, *Phys. Rev. B: Condens. Matter Mater. Phys.*, 1974, **10**, 1298.

4 T. H. Le, A. Nafady, X. Qu, A. M. Bond and L. L. Martin, *Anal. Chem.*, 2012, **84**, 2343.

5 M. R. Suchanski and R. P. Van Duyne, *J. Am. Chem. Soc.*, 1976, **98**, 250.

6 (*a*) B. F. Abrahams, T. A. Hudson and R. Robson, *Cryst. Growth Des.*, 2008, **8**, 1123; (*b*) B. F. Abrahams, R. W. Elliott, T. A. Hudson and R. Robson, *Cryst. Growth Des.*, 2010, **10**, 2860; (*c*) B. F. Abrahams, R. W. Elliott, T. A. Hudson and R. Robson, *CrystEngComm*, 2012, **14**, 351.

7 B. F. Abrahams, R. W. Elliott, T. A. Hudson and R. Robson, *Cryst. Growth Des.*, 2013, **13**, 3018.

8 T. H. Le, J. Lu, A. M. Bond and L. L. Martin, *Inorg. Chim. Acta*, 2013, **395**, 252.

9 T. A. Hudson and R. Robson, *Cryst. Growth Des.*, 2009, **9**, 1658.

10 (*a*) T. J. Kistenmacher, T. J. Emge, A. N. Bloch and D. O. Cowan, *Acta Crystallogr., Sect. B: Struct. Sci.*, 1982, **38**, 1193; (*b*) K. Bechgaard, T. J. Kistenmacher, A. N. Bloch and D. O. Cowan, *Acta Crystallogr., Sect. B: Struct. Sci.*, 1977, **33**, 417.

11 D. A. Dixon, J. C. Calabrese and J. S. Miller, *J. Phys. Chem.*, 1989, **93**, 2284.

12 T. J. Emge, T. M. Maxfield, D. O. Cowan and T. J. Kistenmacher, *Mol. Cryst. Liq. Cryst.*, 1981, **65**, 161.

13 (*a*) S. A. O'Kane, R. Cérac, R. H. Zhao, X. Ouyang, J. R. Galán-Mascarós, R. Heintz and K. R. Dunbar, *J. Solid State Chem.*, 2000, **152**, 159; (*b*) M. Meneghetti and C. Pecile, *J. Chem. Phys.*, 1986, **84**, 4149.

14 J. Tauc, *Mater. Res. Bull.*, 1968, **3**, 37.

15 E. L. Martin, Fluoro and Cyano-Substituted 7,7,8,8-Tetracyanoquinodimethans and Intermediates Thereto, *U.S. Patent*, 3,558,671, 1971.

16 G. M. Sheldrick, *Acta Crystallogr., Sect. A: Found. Crystallogr.*, 2008, **64**, 112.

17 L. J. Farrugia, *J. Appl. Crystallogr.*, 1999, **32**, 837.